RSC Advances

ROYAL SOCIETY OF CHEMISTRY

www.rsc.org/advances

Table of Contents

Anion Exchange Membranes by Bromination of Benzylmethyl-Containing Poly(arylene ether)s for Alkaline Membrane Fuel Cells

Xiuhua Li, [*,a, b] Shanshan Cheng,[a, b] Liuchan Wang,[a, b]Qiang Long,[a, b]Jinxiong Tao[a, b] Guanghui Nie,[a, b]Shijun Liao[a, b]

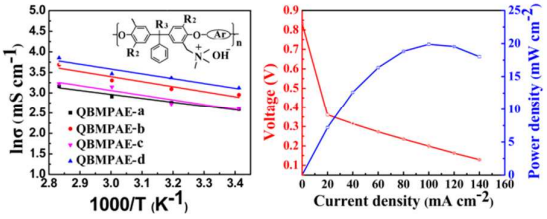

Fast and safe fabrication of anion exchange membranes started with the bromination of poly(arylene ether)s containing tetramethyl triphenyl methane moieties.

Cite this: DOI: 10.1039/c0xx00000x

www.rsc.org/xxxxxx

ARTICLE TYPE

Anion exchange membranes by bromination of benzylmethyl-containing poly(arylene ether)s for alkaline membrane fuel cells

Xiuhua Li,[*,a, b] Shanshan Cheng,[a, b] Liuchan Wang,[a, b] Qiang Long,[a, b] Jinxiong Tao[a, b] Guanghui Nie,[a, b] Shijun Liao[a, b]

Received (in XXX, XXX) XthXXXXXXXXX 20XX, Accepted Xth XXXXXXXXX 20XX
DOI: 10.1039/b000000x

Functionalized quaternary ammonium poly(arylene ether)s (QBMPAEs) containing tetramethyl triphenyl methane moieties are synthesized via polycondensation, benzylic bromination, quaternization, and alkalization. The structures of the QBMPAEs ionomers have been confirmed by ^{1}H NMR. The water uptakes, ion exchange capacities (IEC), hydroxide ion conductivities, and mechanical properties, as well as the thermal and chemical stabilities of the QBMPAEs membranes have been assessed. The IECs of the ionomers range from 0.90 to 1.73 mmolg^{-1} and can be controlled via the conditions of the bromination reaction. The hydroxide ion transport activation energy (Ea) of the QBMPAEs membranes varies from 8.01 to 10.02 kJ mol^{-1}. The QBMPAE-**d** membrane with an IEC value of 1.73 mmol g^{-1} bears a sulfone/ketone structure and demonstrates the highest conductivity (46.6 mS cm^{-1}) at 80 ℃. The QBMPAE-**d** membranes conditioned in 1~10 M NaOH at room temperature for 30 days display conductivity higher than that of the parent membrane. An H_2/air single fuel cell with a membrane electrode assembly (MEA) made entirely in-house from QBMPAE-**d** achieves a peak power density of 20.1 mW cm^{-2} with 0.1 mg (Pt) cm^{-2} of the anode and 0.2 mg (Pt) cm^{-2} of the cathode at 70 ℃. The properties of the ionomers membranes demonstrate their potential applications in alkaline fuel cells.

1. Introduction

Due to the growing energy crisis and problems with environmental pollution, exploring and developing clean or renewable energy sources has been prioritized by nearly every country in the world. Fuel cells have been universally accepted as clean energy sources for the 21st century.[1,2] Recently, anion exchange membrane fuel cells (AEMFCs) have attracted significant attention because they have advantages over proton exchange membrane fuel cells (PEMFCs), such as fuel flexibility, reduced fuel crossover, and high fuel cell efficiency.[3] In particular, the faster oxygen reduction kinetics in alkaline fuel cells enables the use of non-noble metals (Ag, Co, or Ni) as catalysts, reducing the cost of the fuel cells.[4]

Anion exchange membranes (AEM) with functional groups capable of transporting the hydroxyl anions are some of the key materials in AEMFCs. Because state-of-the-art AEMs cannot satisfy the requirements of AEMFCs, much effort has been spent developing better AEM materials. Three types of AEMs, including hybrid, polymer composite and homogeneous membranes, have been reported. Hybrid membranes combine the advantages of both organic and inorganic materials; examples include PVA-SiO_2 hybrid composites,[5,6] PEO-SiO_2 hybrid composites,[7] PVA-ZrO_2-KOH hybrid composites,[8] and poly(arylene ether sulfone)-ZrO_2 composites.[9] Polymer composite membranes have inter-penetrating networks of chemically modified hydrophobic/hydrophilic polymers. The hydrophobic polymers provide good thermal, chemical and mechanical properties, while the hydrophilic conductive polymers transport anions. Recently, a series of polymers composites membranes based on PVA and other polymers have been revealed, including the cross-linked PVA/QHECE,[10] PVA/PDDA,[11] and PVA/PAADDA/PEG.[12] These membranes show good stability against alkali and oxidation, but they have poor ionic conductivity. Most of these membranes display several mS cm^{-1},and the best candidate shows a conductivity of 25 mS cm^{-1}. The homogeneous membranes are made from an exclusive conductive polymer material with cationic groups covalently bound to the polymer backbones. Mobile counter anions, such as OH^-, are associated with each cationic group. Homogeneous membranes have been extensively explored. AEMs based on poly(arylene ether sulfone),[13-16] polyethersulfone cardo,[17] poly(ether-imide),[18] poly(phthalazinone ether ketone),[19] poly(arylene ether ketone),[20-23] poly(phenylene),[24] poly(aryl ether oxadiazole),[25] polystyrene(ethylene butylenes)s,[26] poly(phenylene oxide),[27,28] poly(ethylene-co-tetrafluoroethylene),[29] and poly(fluorenyl ether ketone sulfone),[30] have been reported. Poly(arylene ether)s are the focus of many investigations due to

[a]*School of Chemistry & Chemical Engineering, South China University of Technology, Guangzhou 510641, P. R. China.*
Fax: +86-20-2223-6591; Tel:+86-20-2223-6591;
E-mail: lixiuhua@scut.edu.cn
[b]*The Key Laboratory of Fuel Cell Technology of Guangdong Province, South China University of Technology, Guangzhou 510641, P. R.China.*

their excellent chemical and thermal stabilities, outstanding membrane features, and good solubility in organic solvents. Until now, most AEMs have been obtained by reacting a tertiary amine with the benzylic chloromethyl groups attached to the polymer backbone; these groups were installed by chloromethylating the parent polymers.[13-20] However, the chloromethylation reaction is highly undesirable due the toxicity and carcinogenicity of chloromethyl methyl ether. Moreover, chloromethylation reactions often require long reaction times and large excesses of reagents. This method is time-consuming and lacks atom economy. Therefore, finding safer and faster approaches for fabricating anion exchange membranes with stable backbones and cationic groups is urgent.

Brominating benzylmethyl groups is a promising and green method used to prepare AEMs. Xu and Yang reported AEMs based on the reaction between poly(2,6-dimethyl-1,4-phenylene oxide) and bromine.[31] Due to the irritating and toxic nature of bromine, this method is semi-green. Hickner et al. generated AEMs deriving by functionalizing of methyl-containing poly(sulfone)s using NBS for radical bromination. Compared to chloromethylation, bromination is faster (several hours versus several days), more efficient (80-95% according to the amount of bromination reagent added), and more specific; bromine, and therefore quaternary ammonium groups, can be introduced to specific locations on the polymer chain.[32] In previous work, we have introduced chloromethyl groups into tetramethyl triphenyl methane-based polymers via chloromethylation as the precursors for quaternary ammonium groups. These methyl groups are the placeholders that ensure functionalization at the electron-rich positions. The obtained quaternized poly(arylene ether)s (QPAEs) show high hydroxide ion conductivities as well as good chemical and thermal stabilities.[33] The tetramethyl triphenyl methane based polymers have a high density due to the four benzylmethyl groups in each repeat unit that can be brominated. Further functionalization can afford AEMs with higher IECs and new architectures. In this paper, we report a series of AEMs derived from brominated tetramethyl triphenyl methane based polymers. The titular quaternized membranes were obtained by soaking the brominated polymer membranes in an aqueous trimethylamine solution. The AEMs were assessed in terms of their water uptake, swelling ratio, hydroxide conductivity, mechanical properties, and single fuel cell performance, as well as their thermal and chemical stability.

2. Experimental Section

2.1 Materials

Bis(3,5-dimethyl-4-hydroxyphenyl)-phenyl methane (BDHPM) and 1,4-bis(4-fluorobenzoyl) benzene (BFBB) were synthesized according to Wang.[34] 4,4'-Difluorodiphenyl sulfone (FPS), 4,4'-Difluorobenzophenone (DFBP) were purchased from TCI, recrystallized from toluene and dried under vacuum before use. Potassium carbonate was dried under vacuum oven at 120 ℃ for 24 h before use. *N*,*N*-dimethylacetamide (DMAc), toluene were treated with 4 Å molecular sieves before use. N-bromosuccinimide (NBS), 2,2-azobis(isobutyronitrile) (AIBN), sodium hydroxide, potassium carbonate (K_2CO_3), 1,1,2,2-tetrachloroethane, chloroform, methanol, toluene, trimethylamine aqueous solution (33 wt%) were obtained from commercial sources and used as received.

2.2 Synthesis of poly(arylene ether)s (PAEs)

A series of parent polymers poly(arylene ether)s containing tetramethyl triphenyl methane (PAE-**a** to PAE-**d**) were synthesized via nucleophilic substitution polycondensation. A typical polymerization procedure for PAE-**a** was as follows: BDHPM (0.9973 g, 3 mmol), FPS (0.7628 g, 3 mmol), potassium carbonate (0.621 g, 4.5 mmol), DMAc (6 mL) and toluene (10 mL) were added to a 50 mL three-necked, round-bottomed flask equipped with a Dean-stark trap, a condenser, a nitrogen inlet/outlet, and a magnetic stirrer. The mixture was heated at 145 ℃ for 4 h under nitrogen to remove water via azeotropic reflux; afterward, the toluene was removed. The reaction mixture was heated to 175 ℃ for 8 h. After cooling, the mixture was diluted with 15 mL of additional DMAc. The polymer was isolated via precipitation in 100 mL of methanol containing 2 mL of concentrated HCl; the product was washed with deionized water several times and dried under vacuum. After drying, the crude product was cleaned of inorganic salts by filtering through a thin layer of celite after dissolution in 30 mL of chloroform. Then, the polymer was precipitated in 300 mL of methanol with rapid stirring. Finally the fiber-like polymer was dried at 80 ℃ under vacuum for 24 h to give PAE-**a**. PAE-**b** to PAE-**d** were prepared using the same procedure.

2.3 Bromination of poly(arylene ether)s

A typical bromination procedure for the poly(arylene ether)s (PAEs) is as follows. First, PAE-a (1.6392 g, 3 mmol) was dissolved in 30 mL of 1,1,2,2-tetrachloroethane in a 100-mL, three-necked flask equipped with a magnetic stirrer and a condenser under nitrogen. The mixture was stirred until PAE-**a** was fully dissolved. Afterward, NBS (1.3883 g, 7.8 mmol) and AIBN (0.0821 g, 0.5 mmol) were added to the solution. The reaction mixture was heated to 85 ℃ to obtain a red-brown transparent solution. After 4 h, the mixture was cooled to room temperature and coagulated in methanol with vigorous stirring. The precipitate was washed with methanol several times and dried under vacuum at 80 ℃ for 24 h, obtaining a yellow fibrous polymer (BMPAE-**a**). BMPAE-**b** through BMPAE-**d** were synthesized using a similar procedure.

2.4 Membrane preparation, quaternization and alkalization

The brominated poly(arylene ether)s (BMPAEs) (1 g) were dissolved in 1,1,2,2-tetrachloroethane (10 mL). The solutions were filtered, cast onto flat glass plates, and heated (60 ℃) for 24 h to remove residual solvent. Afterward, the membranes were peeled off and immersed in 33% aqueous trimethylamine for 48 h at room temperature, generating the quaternized membranes. After several washes with deionized water, the membranes were immersed in 1 M NaOH for 48 h at room temperature to change the counter anion from bromide to hydroxide. After alkalization, the quaternized membranes were washed thoroughly with deionized water to remove residual NaOH. The QBMPAEs membranes were soaked in deionized water in a closed vessel at least 24 h before analysis.

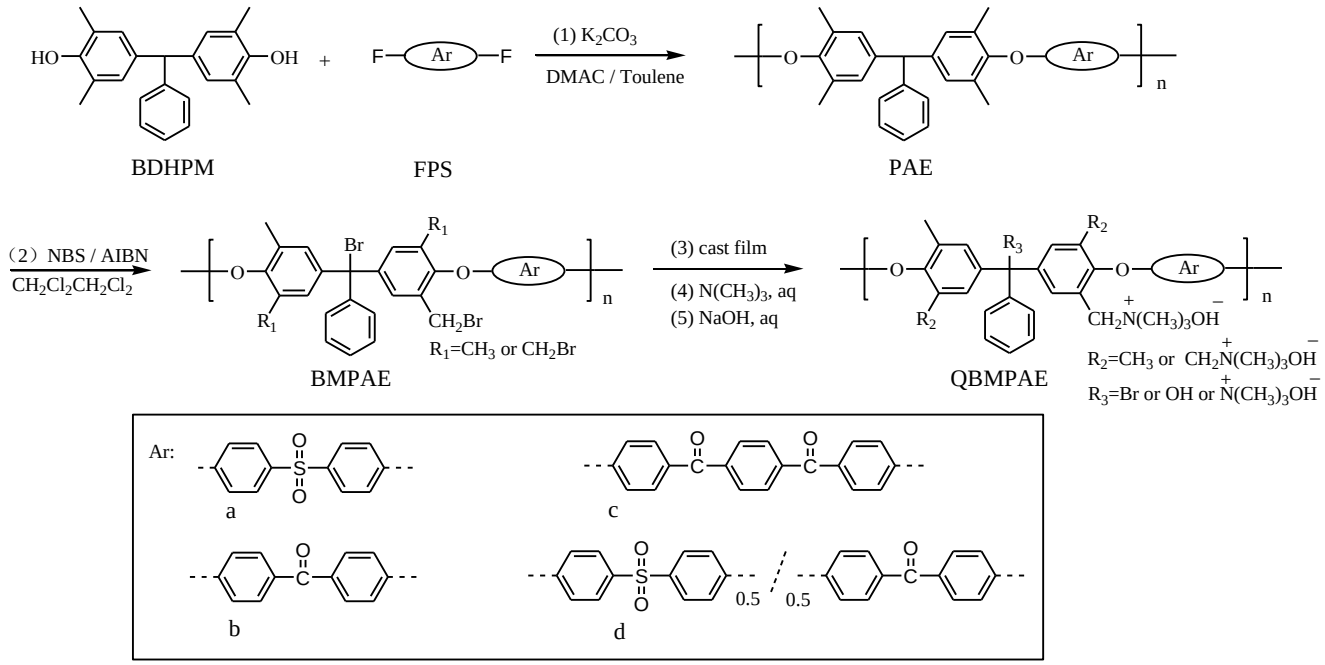

Scheme 1 Synthesis route for the poly(arylene ether)s ionomers: (1) polymerization, (2) bromination, (3) membrane preparation, (4) quaternization and (5) alkalization

2.5 Characterization

2.5.1 ^{1}H-NMR, FT-IR, TGA,GPC and Mechanical Properties

The ^{1}H NMR spectra were measured with a Bruker AVANCE 400S in deuterated chloroform ($CDCl_3$) or dimethyl sulfoxide (DMSO-d_6) with tetramethylsilane (TMS) as an internal reference. The thermogravimetric analyses (TGA) were conducted with a TAINC SDT Q600 thermogravimetric analyzer under a protective nitrogen atmosphere (100 mL min^{-1}), at 10 ℃ per minute from 35 to 700 ℃. Gel permeation chromatography (GPC) was carried out on a Waters 510 HPLC equipped with 5 μm phenol gel columns (linear, 4×500 Å) arranged in series while using chloroform as a solvent, a UV detector at 254 nm and standard polystyrenes (Shodex STANDARD SM-105) as standards. The system was operated at 25 ℃ and 1 mL min^{-1}. The mechanical properties of the membranes were measured with a SANS Electromechanical Universal Testing Machine (UTM6000) at 25 ℃ and 100% RH when stretching at 50 mm min^{-1}. The data were evaluated using SANS Power Test-SOOC software.

2.5.2 Water uptake and swelling ratio

A piece of QBMPAEs membranes was immersed in degassed deionized water at a known temperature for 24 h. The wet membrane was quickly wiped with tissue paper and weighed to obtain the wet weight (W_{wet}). Afterward, the membrane was dried at 60 ℃ under vacuum for 24 h to obtain a constant weight (W_{dry}). The water uptake of the membrane was calculated:

$$water\ uptake = \frac{W_{wet} - W_{dry}}{W_{dry}}$$

The swelling ratio (SR) of the membrane was calculated using the change in the film length between the dry and wet membrane:

$$swelling\ ratio = \frac{L_{wet} - L_{dry}}{L_{dry}}$$

where L_{wet} was the length of the wet membrane after immersion in deionized water at a known temperature for 24 h, and L_{dry} was the length of the dry membrane.

The measurements were taken using five samples for each type of QBMPAE membrane. The average values were recorded as the water uptake and SR.

2.5.3 Ion exchange capacity (IEC)

The IEC of the QBMPAE membrane (Br^- form) was determined using Mohr titration. Approximately 0.2 g of membrane (Br^- form) was immersed in 50 mL of 0.2 M $NaNO_3$ for 24 h and titrated with 0.01 M $AgNO_3$ with K_2CrO_4 as colorimetric indicator. The IEC was calculated:

$$IEC_{Br^-} = \frac{M_{AgNO_3} V_{AgNO_3}}{W_{dry}}$$

where M_{AgNO3} (M) and V_{AgNO3} (mL) are the concentration and consumed volume of the $AgNO_3$ solution, and W_{dry} (g) is the weight of the dry QBMPAE membrane (Br^- form).

The IEC of the QBMPAE membrane (OH^- form) was measured using back titration. The QBMPAE membrane was immersed in 50 mL of a standard HCl (0.01 M) for 4 h. After ion exchange, the HCl mixture was titrated with a standard NaOH (0.01 M) solution with phenolphthalein. Afterward, the membranes were vacuum-dried at 60 ℃ for 24 h to obtain a constant weight. The

IEC values were calculated according to our previous work:[33]

$$IEC_{OH^-} = \frac{M_1V_1 - M_2V_2}{W_{\mathrm{dry}} - (M_1V_1 - M_2V_2)(M_{Cl^-} - M_{OH^-})}$$

where M_1 (M) and V_1 (mL) are the concentration and volume of the initial HCl solution. M_2 (M) and V_2 (mL) are the concentration and volume of the standardized NaOH solution. W_{dry} (g) is the weight of the dry QBMPAE membrane, M_{Cl^-} and M_{OH^-} are the molar masses of Cl^- and OH^-.

2.5.4 Ion conductivity

The QBMPAE membrane was hydrated in deionized water for 24 h. The through plane ion conductivity was measured using a 10 mV oscillating voltage from 1 MHz to 1 KHz using a two-electrode AC impedance method with an IviumStat frequency response analyzer. The samples were fixed between a pair of stainless steel electrodes and immersed in degassed deionized water at 20, 40, 60 and 80 ℃. After each measurement, the degassed deionized water was replaced. The ion conductivity was calculated:

$$\sigma = \frac{l}{RA}$$

where l (cm) is the membrane thickness, R (Ω) is the resistance of the membrane and A (cm^2) is the area of the electrode on the membrane.

2.5.5 Chemical stability test

The chemical stability of the QBMPAEs membranes was explored by immersing them in 1 M NaOH at 60 ℃ for 168 h. Afterward, the hydroxide conductivity and mechanical properties were measured.

The long-term chemical stability of the QBMPAEs membranes was investigated by immersing the membranes in various NaOH solutions (1~8 M) at room temperature for 30 days (720 h). Afterward, the hydroxide ion conductivity was measured at 60 ℃ at a known time after the complete removal of residual NaOH.

2.5.6 Membrane electrode assembly (MEA) fabrication and single-cell performance measurements

An MEA with a 5.0 cm^2 active area was fabricated using a catalyst spraying method. The catalyst ink was prepared by mixing 40% Pt/C (Johnson Matthey) with 5wt% QBMPAE-**d** (IEC= 1.73 mmol g^{-1}) in ethanol and sonicating the mixture for 30 min to obtain a homogeneous solution. Then, the inks were sprayed at defined 5 cm^2 areas on both sides of the QBMPAE-**d** membrane to form catalyst layers with Pt loadings of 0.1 mg cm^{-2} for the anode and 0.2 mg cm^{-2} for the cathode. The polarization curves of the H_2/air single-fuel cells were obtained with fuel cell test stations (Arbin Instruments, USA). Pure hydrogen and air were supplied to the anode and cathode channels at 300 and 800 mL min^{-1}, respectively, through a humidifier maintained at 70 ℃ under 30 psig.

3. Results and Discussion

Table 1 Molecular weights of the parent PAEs measured by GPC

PAE	M_n (kg mol^{-1})	M_w (kg mol^{-1})	M_w/M_n
PAE-**a**	109	187	1.7
PAE-**b**	97	204	2.1
PAE-**c**	116	226	1.9
PAE-**d**	108	212	1.9

3.1 Synthesis and characterization of the parent poly(arylene ether)s (PAEs) and brominated poly(arylene ether)s (BMPAEs)

The parent poly(arylene ether)s (PAEs) were synthesized via nucleophilic substitution polycondensation between bis(3,5-dimethyl-4-hydroxyphenyl)-phenyl methane and difluoro-monomers using potassium carbonate in dry *N*,*N*-dimethylacetamide (DMAc), as shown in Scheme 1(1). The PAEs were obtained as white fibers. The molecular weights of the PAEs were measured using GPC and summarized in Table 1. The M_n and M_w of the PAEs exceed 97 kg mol^{-1} and 187 kg mol^{-1}, respectively. The PAEs are soluble in organic solvents, such as chloroform, dichloromethane, DMAc, 1,1,2,2-tetrachloroethane, *N*,*N*-dimethylformamide (DMF), dimethyl sulfoxide (DMSO) and sulfolane.

To date, most AEMs have been based on precursors generated via chloromethylation.[13-20] Currently, few works have brominated polymers containing benzylmethyl side groups.[21-25,30] The bromination occurs via radical substitution of active hydrogens in benzylmethyl groups attached to the polymer backbones while using a radical initiator and NBS as the bromination reagent. The concentration of active centers is very low compared to chloromethylation. The crosslinking reaction occurring through macromolecular radical coupling is prevented by the low radical concentration and steric hindrance. During chloromethylation, the gelation side reaction is difficult to avoid because the substrate is highly active toward Friedel–Crafts alkylation by the benzylmethyl chloride groups due to the presence of a Lewis acid catalyst and the high density of reaction centers. Obviously, the formation of bromomethyl groups through the quick, selective bromination of methyl groups attached to aryl rings in the polymer is superior. The limited availability of the benzylmethyl-containing polymers prevents the wide spread use of bromination. Bromination is one of the most critical steps toward fabricating AEMs based on benzylmethyl-containing poly(arylene ether)s because this process controls the amount and the reactivity of the bromomethyl groups attached to the polymer. Due to the high reactivity of the tethered bromomethyl groups, the polymer can be readily functionalized with quaternary ammonium groups via quaternization and alkalization.[32] The hydroxide conductivity and the mechanical strength of the fabricated ionomer membranes depend on the amount of quaternized ammonium groups. However, over-bromination results in extensive functionalization and excess water uptake, leading to membrane swelling and uncontrolled deformation. These effects preclude applications for the membrane materials in AEMs. The bromomethyl groups were obtained by the radical substitution of active hydrogens on the benzylmethyl groups attached onto tetramethyl triphenyl methane moieties while using NBS as the bromination reagent and AIBN as the initiator. To obtain a membrane with balanced properties, the bromination conditions, including the dose of the bromination

Table 2 Reaction conditions and results for the PAE brominations

Run	PAE	Molar of NBS (equiv. to PAEs)	Reaction temperature (^{o}C)	Reaction time (h)	DBM
1	PAE-**a**	3.00	85	2	1.43
2		2.80	85	2	1.30
3		2.60	85	4	1.21
4		2.50	85	2	0.94
5		2.00	85	2	0.78
6	PAE-**b**	3.00	85	2	1.42
7		2.60	85	4	1.36
8		2.00	85	2	0.79
9	PAE-**c**	2.60	85	4	1.42
10		2.00	85	2	0.82
11	PAE-**d**	2.90	85	2	1.40
12		2.90	85	4	1.56
13		2.90	85	6	1.53
14		2.60	85	4	1.38
15		2.00	85	2	0.82

Table 3 Molecular weights of the BMPAEs as measured by GPC

BMPAE/DBM	M_n (kg mol^{-1})	M_w (kg mol^{-1})	M_w/M_n
BMPAE-**a**/1.21	89	152	1.7
BMPAE-**b**/1.36	77	150	1.9
BMPAE-**c**/1.42	93	171	1.8
BMPAE-**d**/1.38	71	150	2.1

reagent and the reaction time, were investigated. The degree of bromination (DBM) is the average number of bromomethyl groups per repeating unit of PAE; this value was determined using ^{1}H NMR. The results for the PAEs are summarized in Table 2. We explored effect of time on the bromination of PAE-**d** at an NBS dose of 2.90 and 85 ℃. Initially, the DBM increased over time. Later, the time effect leveled off, and DBM remained constant at 6 h. At 4 h, the brominations were considered complete for the other types of PAEs. Generally, the DBM depended on the ratio of NBS to PAE and increased when increasing the feed ratios and reaction time. The bromomethylated PAEs (BMPAEs) with varying DBMs were synthesized by tuning the ratio NBS to PAEs and reaction time. The molecular weights of the BMPAEs with high DBMs were measured using GPC and are listed in Table 3. The M_n and M_w of the BMPAEs exceed 71 kg mol^{-1} and 150 kg mol^{-1}, respectively. The polydispersity indexes of the BMPAEs were very close to those of the PAEs. The BMPAEs membranes generated from the cast solutions were very tough and ductile. No obvious degradation occurred during the bromination, and the obtained BMPAEs had very high molecular weights.

Fig. 1 (a) and (b) show the ^{1}H NMR spectra of PAE-**a** and BMPAE-**a**. The signals in the ^{1}H NMR spectrum for PAE-**a** (Fig. 1 (a)) were assigned as follows. The signal at approximately 2.05 ppm was attributed to the methyl protons (**a**). The signals above 6 ppm were assigned to the aryl hydrogen atoms (**b, d, e, f, g, h**), except for the signal at 7.26 ppm ($CDCl_3$). The signal at 5.44 ppm was attributed to the tertiary hydrogens (**c**) in the tetramethyl triphenyl methane moieties. In the ^{1}H NMR spectra of BMPAE-**a** (Fig. 1 (b)), the signals contributed by the methyl protons (**a**) were weakened after bromination. The new signals at 4.29 ppm were assigned to the bromomethyl protons (**i**). The other distinct change is that signal **c** at 5.44 ppm disappeared because the tertiary hydrogens were completely replaced by the bromine atoms; these atoms were more active than the primary benzyl hydrogens. Introducing bromomethyl groups onto the polymer chains altered several shifts between 6.8 and 7.5 ppm; these signals were assigned to the triphenyl methane moieties. The DBM was calculated according to a published method:[21]

$$DBM = \frac{12H_i}{3H_i + 2H_{a'}}$$

where H_i is the integral of brominated methyl protons, and $H_{a'}$ corresponds to the peak area of remaining methyl protons.

3.2 Preparation of quaternized poly(arylene ether)s (QBMPAEs) membranes

The BMPAEs were dissolved in 1,1,2,2-tetrachloroethane with stirring. The membranes were fabricated using a solution casting process. The membranes were dried under vacuum at 60 ℃ for 24 h to remove residual solvent. Afterward, they were immersed in 33 wt% aqueous trimethylamine for approximately 48 h at room temperature, forming the quaternized membranes (Scheme 1 (4)). After washing with deionized water, the membranes were immersed in 1 M sodium hydroxide to convert the bromide to hydroxide (Scheme 1(5)). The quaternized membranes became hydrophilic and swollen. DBM is an important factor when fabricating quaternized membranes. Overly high DBM values can generate swollen membranes and render solubility in trimethylamine solutions. QBMPAEs membranes with suitable hydrophilicity were obtained by functionalizing the BMPAEs with suitable DBMs. The QBMPAEs membranes were clear, light yellow and tough. The QBMPAEs ionomers are soluble in some common organic solvents such as methanol, ethanol, DMAc, N,N-dimethylformamide (DMF), dimethyl sulfoxide (DMSO) and sulfolane. The QBMPAEs were examined using ^{1}H NMR. Fig. 1(c) shows the ^{1}H NMR spectrum of QBMPAE-**a**. The sharp signals for the bromomethylene protons (**i**) at 4.29 ppm in the ^{1}HNMR spectrum of BMPAE-**a** (Fig. 1 (b)) became a broad signal at 4.31 ppm in for QBMPAE-**a** (Fig. 1(c)) due to the

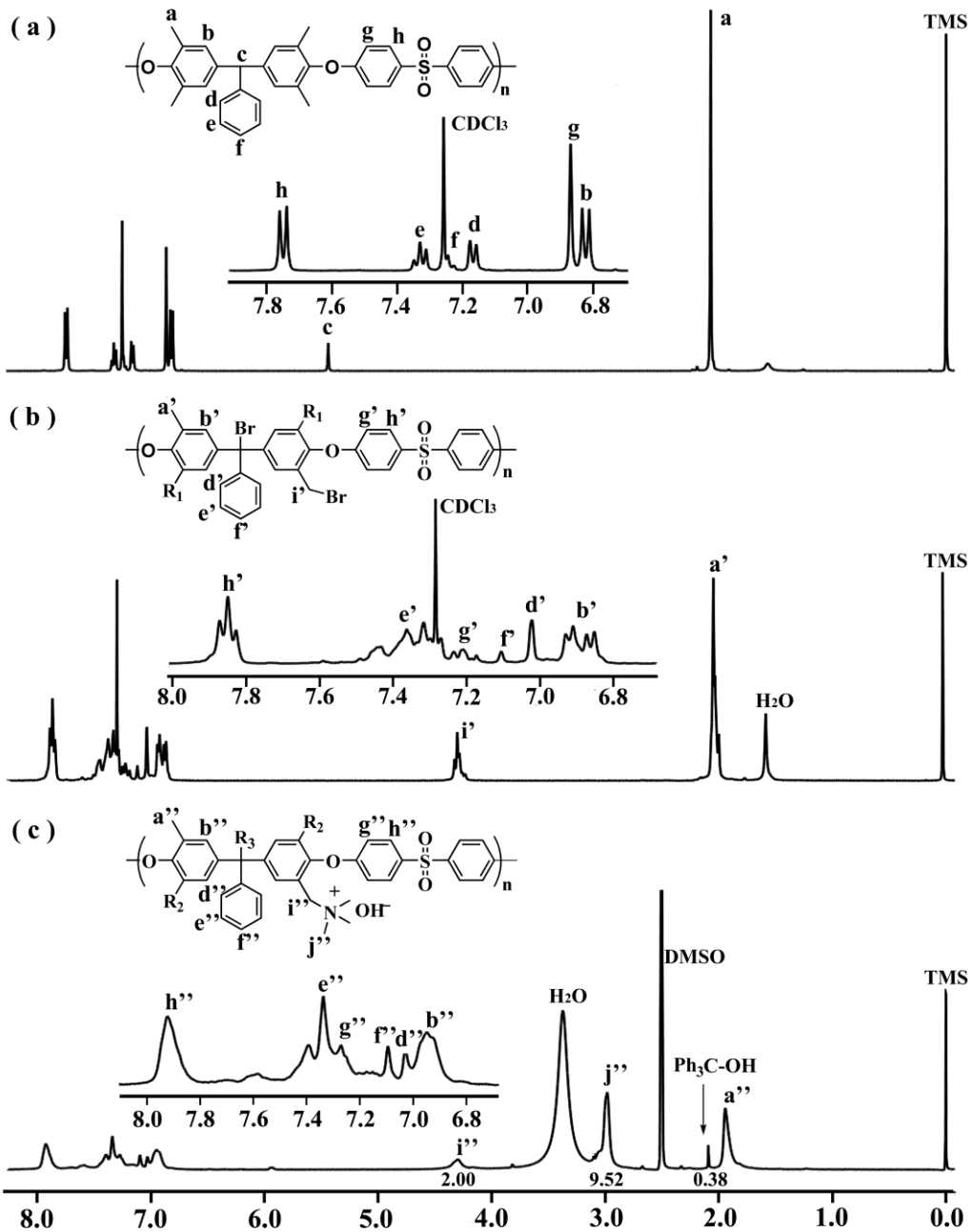

Fig. 1 The ^{1}H NMR spectra of (a) PAE-a, (b) BMPAE-a, and (c) QBMPAE-a.

strong electron withdrawing effect of the quaternized ammonium groups. The new multiplet at 3.00 ppm is assigned to the methyl protons (**j**) of the quaternized ammonium groups. The ratio of the ammonium methyl group protons (**j**) to the methylene moieties protons (**i**) (9.52:2) is higher than that of the theoretical ratio (9:2) because the triphenyl methyl bromide groups participate in the quaternization. However due to the steric hindrance of the triphenyl methyl bromide groups, hydrolysis is more competitive than quaternization in 33wt% aqueous trimethylamine. The new signal at 2.10 ppm is assigned to an aliphatic hydroxyl group. The ratio of the hydroxyl group to methylene protons is 0.38:2, supporting the conjecture. When assuming complete quaternization of the triphenyl methyl bromide groups, the theoretical ratio of the ammonium methyl group protons to the methylene moieties protons is 11.25:2. The disparity between the calculated and theoretical values indicate that the triphenyl methyl bromide groups rarely quaternized and can therefore be ignored during the theoretical calculations for IECs and the incomplete quaternization of the side bromomethylene groups.

3.3 Ion exchange capacity (IEC), water uptake, swelling ratio and hydroxide conductivities of QBMPAEs membranes

The IEC, water uptake and swelling ratios of the QBMPAEs membranes are listed in Table 4. The theoretical IEC values were calculated using the DBMs derived from the BMPAE ^{1}H NMR data after assuming complete functionalization. The experimental

IEC values were obtained via back titration. The experimental IEC values are all lower than the theoretical ones due to incomplete functionalization. The ^{1}H NMR data for the QBMPAEs (Fig. 1(c)) strongly support this conjecture. The primary contributors to the incomplete functionalization are the bromomethylated moieties surrounded by hydrophobic segments inside of the BMPAEs membranes. Because quaternization occurred in solid membranes rather than solutions, the bromomethylated segments that are surrounded by hydrophobic segments inside the BMPAEs membranes are unlikely to interact with the aqueous trimethylamine, leading to incomplete quaternization. The experimental IEC values for the QBMPAEs membranes (Br^- form) are listed in Table 4 to estimate the degree of quaternization and the transportation number for OH^- in the membranes. The degree of quaternization was calculated from the ratio of the experimental IEC value for the QBMPAEs membranes (Br^- form) to the theoretical value from the DBM. The degrees of quaternization in the QBMPAEs membranes (Br^- form) ranged from 93% to 98%. Incomplete bromide ion exchange under certain conditions due to the equilibrium of the reversible ion exchange reaction may have also contributed to incomplete functionalization. The molar ratio of OH^- to Br^- in the QBMPAEs membranes was calculated using the ratio of the experimental IEC values of the QBMPAEs membranes (OH^- form) to the experimental IEC values of the QBMPAEs membranes (Br^- form); this value exceeded 91/9, indicating that the degree of ion exchange exceeded 91%. In general, the estimated degree of functionalization for the QBMPAEs membranes exceeded 81%. The experimental values determined from the ratio of the experimental IEC values for the QBMPAEs membranes (OH^- form) to the theoretical IEC values from the DBMs ranged from 85.7 to 93.3%. The estimated values agree well with the experimental results.

Water uptake was a key parameter for ion-exchange membrane due to the strong dependence of the hydroxide conductivity and mechanical properties of AEMs on the water content.[35] A membrane containing adequate water can provide additional active transport channels for anions and show higher hydroxide conductivity. However, excess water leads to over-swelling. In extreme cases, the uncontrollable deformation precludes the membranes as candidates for AEMs. As shown in Table 4, the DBMs for all BMPAEs except BMPAE-c must remain lower than 1.4. The QBMPAEs membranes based on the BMPAEs with the highest DBMs dissolve in aqueous trimethylamine, precluding their use as AEMs. PAE-**c** can be loaded at a slightly higher DBM due to the high molecular weightof the 1,4-bis(benzoyl) benzene units. Compared to AEMs derived from the same parent backbones through chloromethylation, the QBMPAEs membranes synthesized using bromination showed good hydrophilicity and high water uptakes at similar IECs due to the different locations of the quaternized ammonia groups. The quaternized ammonia in the QBMPAE-based AEMs are very close to strong polar bonds, such as ether, ketone and sulfone bonds, and can therefore bind water through hydrogen bonding. The hydrophilicity of the quaternized ammonia makes the strong polar bonds water-rich, strengthening the hydrogen bonds and providing good hydrophilicity and high water uptake to the QBMPAEs membranes. The quaternized ammonia groups in the AEMs based on CMPAEs occur at the weak polar tetramethyl triphenyl methane moieties far from the strong polar units,[33] limiting the hydrophilicity of the AEMs. The

Table 4 DBM, IEC, water uptake, λ, swelling ratio and hydroxide conductivity of the QBMPAEs membranes

membrane	DBM	IEC (mmol g^{-1})			Water uptake (%)		λ^e		Swelling ratio (%)		Conductivity (mS cm^{-1})	
		thero[a]	expt[b]	expt[c]	T_1[d]	T_2[d]	T_1[d]	T_2[d]	T_1[d]	T_2[d]	T_1[d]	T_2[d]
QBMPAE-**a**	0.80	1.13	—	1.01±0.12	22.9	28.7	12.6	15.7	9.1	11.4	6.2±0.1	12.1±0.1
	1.21	1.68	1.58±0.03	1.45±0.11	41.1	45.0	15.7	17.2	16.2	18.6	13.6±0.2	23.4±0.3
	1.43	1.89	—	—	—	—	—	—	—	—	—	—
QBMPAE-**b**	0.77	1.15	—	1.06±0.14	28.3	32.1	14.8	16.8	10.3	12.5	7.9±0.1	14±0.1
	1.36	1.91	1.86±0.05	1.71±0.15	54.9	62.8	17.8	20.4	30.1	38.1	19.2±0.1	39.8±0.2
	1.42	1.97	—	—	—	—	—	—	—	—	—	—
QBMPAE-**c**	0.8	1.03	—	0.90±0.08	16.3	22.1	10.1	13.6	6.5	11.3	2.2±0.1	5.5±0.1
	1.42	1.75	1.64±0.04	1.50±0.13	30.2	72.8	11.2	26.9	17.7	77.4	13.7±0.1	25.4±0.2
	1.52	1.82	—	—	—	—	—	—	—	—	—	—
QBMPAE-**d**	0.83	1.20	—	1.12±0.16	30.7	32.9	15.3	16.3	10.3	13.8	8.1±0.2	21.5±0.3
	1.38	1.87	1.81±0.02	1.73±0.15	53.1	89.6	17	28.7	29.3	55.8	22.5±0.1	46.6±0.4
	1.48	1.99	—	—	—	—	—	—	—	—	—	—

[a] Calculated from the polymer composition and DBM; [b] IEC for QBMPAEs membranes (Br^- from), determined using Mohr titration; [c] IEC for QBMPAEs membranes (OH^- from), determined using back titration; [d] T_1 = 20 °C, T_2 = 80 °C. [e] λ = [water uptake (g g^{-1})/18.02 (g mol^{-1})] ×[1000/IEC (mmol g^{-1})].

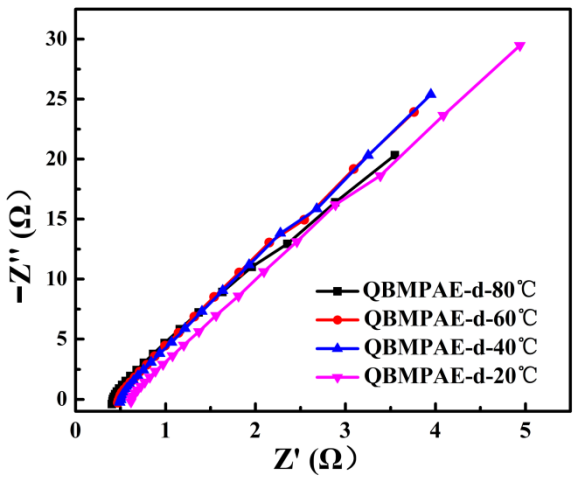

Fig. 2 The electrochemical impedance spectroscopy of QBMPAE-**d** at various temperature.

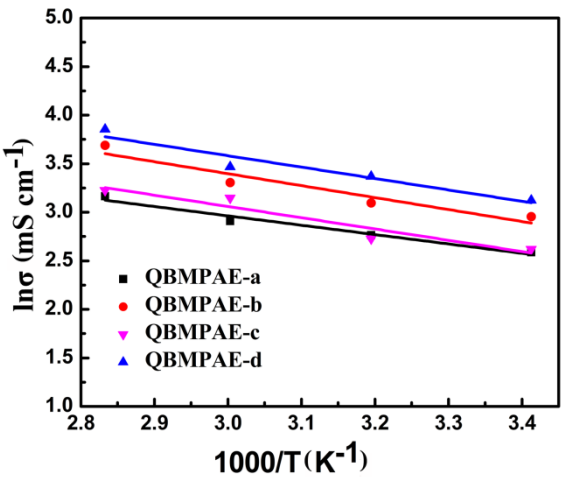

Fig. 3 Arrhenius plots of QBMPAE-**a** (IEC = 1.45 mmol g^{-1}), QBMPAE-**b** (IEC = 1.71 mmol g^{-1}), QBMPAE-**c** (IEC = 1.50 mmol g^{-1}), and QBMPAE-**d** (IEC = 1.73 mmol g^{-1}) membranes at various temperatures.

various trends for water uptake in the QBMPAEs membranes regarding the IECs and temperature are similar to the CMPAE-based AEMs. Water uptakes increases when increasing the IECs and temperature. To explore the relationship between the hydrophilicity and structure of the QBMPAEs membranes, the water molecules bound perammonium group (denoted as λ in Table 4) in the QBMPAEs membranes were calculated. Obviously, the λ values changed imperceptibly when increasing the IEC and temperature on the same backbone. The λ values for QBMPAE-**c** and **d** show a strong temperature dependence at higher IECs. In particular, the QBMPAE-**d** with the highest IEC displayed the highest λ value (28.7) at 80 ℃ because the bulky repeat units containing sulfone moieties generate disorder in the uniformly sequenced ketone backbones, loosening the AEM aggregation and providing more, free volume holding water. This effect enhanced the water uptake conferred by the repeating units containing carbonyl moieties. The swelling ratios of the QBMPAEs membranes depend on the structures and temperature similar to that of λ. The temperature dependence of the swelling ratios for the QBMPAE-**a** and **b** membranes were not as sensitive as that of the QBMPAE-**c** and **d** membranes. The swelling ratio for the QBMPAE-**c** with an IEC of 1.50 mmol g^{-1} at 80 ℃ was several times higher than that at 20 ℃.This large deformation disqualifies QBMPAE-**c** from applications in fuel cells. In general, the QBMPAEs membranes other than QBMPAE-**c** exhibit moderate water uptake, λ values and swelling ratios, as well as excellent dimensional stability.

The through plane ion conductivity was measured using a two-electrode AC impedance method. The electrochemical impedance spectroscopy of QBMPAE-**d** at variuos temperature is shown in Fig. 2. The resistance R of the membranewas derived from the intercept of the high-frequency complex impedance with the Re(Z) axis. The ionic conductivity of the QBMPAEs membranes are listed in Table 4. The conductivity of the QBMPAEs membranes increased significantly with the IEC and temperature. The trends were similar to that of the water uptake. Compared to their counterparts based on CMPAEs, the conductivities of the QBMPAEs membranes improved greatly. The QBMPAEs membranes with the IECs values above 1.45 mmol g^{-1} exhibited more than 10 mS cm^{-1} at 20 ℃ and nearly doubled ionic conductivities at 80 ℃. In particular, the QBMPAE-**d** (IEC = 1.73 mmol g^{-1}) membrane exhibited the highest ionic conductivities (22.5 and 46.6 mS cm^{-1} at 20 ℃ and 80 ℃, respectively), greatly exceeding those of a CMPAE-**d** with the same IEC in the previous work (6.9 and 32.9 mS cm^{-1} at 20 ℃ and 80 ℃, respectively).[33] This improvement is due to the improved water uptake ability, which facilitates the formation of hydroxide ion conductive channels and the movement of hydroxide ions. Due to incomplete alkalization, the contribution of bromide ions should be accounted for. The transportation numbers for OH^- in the membranes were estimated from the molar ratios of OH^- to Br^- and the limiting equivalent ionic conductances of OH^- and Br^- (the relative conductivity of OH^- to Br^- is 2.54) in aqueous solutions.[36] The obtained transportation numbers for OH^- in the QBMPAEs membranes exceeded 0.96, ensuring the hydroxide ion conductivity of the QBMPAEs membranes. During fuel cell operation using hydroxide exchange membrane materials, the hydroxide conductivity must be above10 mS cm^{-1} at working temperatures from 60-90 ℃.[37] Apparently, the QBMPAEs membranes with the IECs values above 1.45 mmol g^{-1} fulfilled this requirement. Fig. 3 shows the temperature dependence for the hydroxide conductivities of the QBMPAEs. The relationship between lnσ (σ is the hydroxide conductivity) and 1000/T (T is the absolute temperature) followed Arrhenius behavior. Therefore, the hydroxide transport activation energy Ea of the membranes could be calculated using the following equation as Varcoe's work[29]:

$$E_a = -b \times R$$

where b is the slope of the regressed linear lnσ−1000/T plots, and R is the gas constant (8.314 J $(mol\ K)^{-1}$). The calculated ion transport activation energies Ea of the various QBMPAEs membranes varied from 8.01 to 10.24 kJ mol^{-1}, as listed in Table 5. Obviously, the Ea values for the QBMPAEs were much lower than that of Nafion-117 (12.75 kJ mol^{-1})[38] and materials based on

Table 5 The hydroxide transport activation energies of the QBMPAEs membranes

QBMPAEs membranes	The hydroxide transport activation energy E_a (kJ mol^{-1})
QBMPAE-**a**	8.01
QBMPAE-**b**	10.24
QBMPAE-**c**	9.56
QBMPAE-**d**	9.76

Table 6 Mechanical properties of the the QBMPAEs membranes

Membrane	IEC[a] (mmol g^{-1})	Tensile strength[b] (MPa)	Tensile modulus[b] (MPa)	Elongation at break[b] (%)
QBMPAE-**a**	1.45±0.11	14.8±0.7	410.6±8.2	45.5±8.2
QBMPAE-**b**	1.71±0.15	9.2±0.5	257.6±21.2	62.1±8.1
QBMPAE-**c**	1.50±0.13	18.6±0.2	298.7±8.3	42.5±7.3
QBMPAE-**d**	1.73±0.15	10.9±0.1	131.7±21.3	84.6±8.4
$PVMImOH_{40}$-DVB_4[38]	1.47±0.08	13.57±1.86	449.12±42.33	51.75±7.96
QBMPAE-c[33]	1.45	17.5±0.4	416.7±3.7	23.4±0.3
BIm-PPO-0.30[27]	1.67	12.3	870	1.0
QPPO[27]	2.19	4.3	330	17.3
ImPPO[27]	2.21	21.7	800	7.2
ETFE-AAEM[29]	1.03±0.11	19.0	\	87
QPE-e[39]	1.56	33.5	550	69
Nafion-117[40]	0.91	21.1	6.6	370.6

[a] Experimental IEC for QBMPAEs membranes (OH^- from), determined using back titration; [b]The samples were measured at 25 °C, 100% RH.

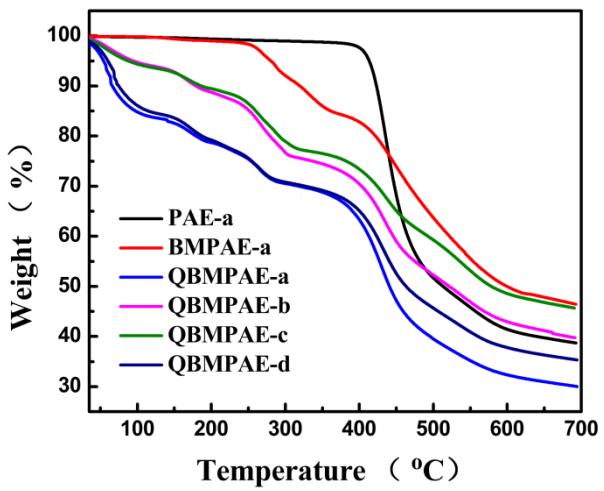

Fig. 4 TGA curves of PAE-**a**, BMPAE-**a**, QBMPAE-**a** (IEC = 1.45 mmol g^{-1}), QBMPAE-**b** (IEC = 1.71 mmol g^{-1}), QBMPAE-**c** (IEC = 1.50 mmol g^{-1}) and QBMPAE-**d** (IEC = 1.73 mmol g^{-1}).

CMPAEs.[33] Therefore, the hydroxide ion mobility in the QBMPAEs membranes is less sensitive to temperature than that of the protons in Nafion-117.

3.4 Mechanical properties of QBMPAEs membranes

The mechanical properties of the QBMPAEs membranes were measured at room temperature and 100% RH. As shown in Table 6, the tensile strengths of QBMPAE-**a, -b, -c, -d** ranged from 9.2 to 18.9 MPa, and the elongations at break varied from 33% to 100.9%. In general, the tensile strengths of the QBMPAEs membranes decreased with increasing IECs due to the plasticizing effect of the absorbed water. A similar phenomenon has been observed in PEMs and AEMs. Due to the effect of the IEC, the mechanical properties of the QBMPAEs membranes are similar to those of some reported AEMs.[27, 29, 33, 38] The QBMPAEs membranes with IEC values above 1.45 mmol g^{-1} demonstrated excellent hydroxide ion conductivity and good mechanical properties.

3.5 Thermal and chemical stability of QBMPAEs membranes

The thermal and chemical stabilities are important criteria for the AEMs used in fuel cells because some AEMs are usually unstable under AEMFC working conditions, such as strong base and elevated temperatures.[40]

The thermal stability of the QBMPAEs membranes was investigated using TGA under nitrogen. Fig. 4 shows the TGA curves for PAE-**a**, BMPAE-**a**, QBMPAE-**a**, QBMPAE-**b**, QBMPAE-**c**, QBMPAE-**d** from room temperature to 700 ℃. The only weight loss stage for PAE-**a** was caused by main-chain decomposition, and the 5% weight loss temperature was above 420 ℃ due to its rigid aromatic backbone. Two stages of weight loss were observed for BMPAE-**a**. The first stage (220 to 400 ℃) involved a weight loss of 14.9% due to the decomposition of the $-CH_2Br$ side groups, matching the theoretical weight percentage of the bromomethylene groups (15.0 wt%) calculated from the corresponding DBM value (1.21). The second stage (400 to 700 ℃) occurred due to the decomposition of the polymer backbone. Three major weight loss stages were observed for the QBMPAE. The first weight loss stage began below 100 ℃ and corresponded to the removal of residual water. The second weight loss stage (130 to 350 ℃) was caused by the degradation of the quaternary ammonium groups, according to Tanaka.[39] The third stage was due to the polymer backbone decomposition beginning at 350 ℃.

The alkaline stability of the QBMPAEs membranes was investigated by measuring the conductivity and mechanical properties after conditioning with 1 M NaOH at 60 ℃ over 168 h. The membranes maintained their toughness and appearance after the measurements. Table 7 compares the hydroxide conductivities of the membranes before and after the stability test. The decreases in conductivity ranged from 17.3% to 40.6%. The chemical structures of the QBMPAEs before and after the stability test were characterized by ^1H NMR. The ^1H NMR spectra of the QBMPAE-**d** membrane are shown in Fig. 5. The stronger, sharper signal at approximately 2.10 ppm was attributed to benzyl alcohol, and the triphenyl alcohol indicated SN_2 substitution at the quaternary ammonium groups. The variations in the mechanical properties of the QBMPAEs membranes during the alkaline stability test are listed in Table 8. The decreasing amplitudes of the QBMPAEs membranes ranged from 20.2% to

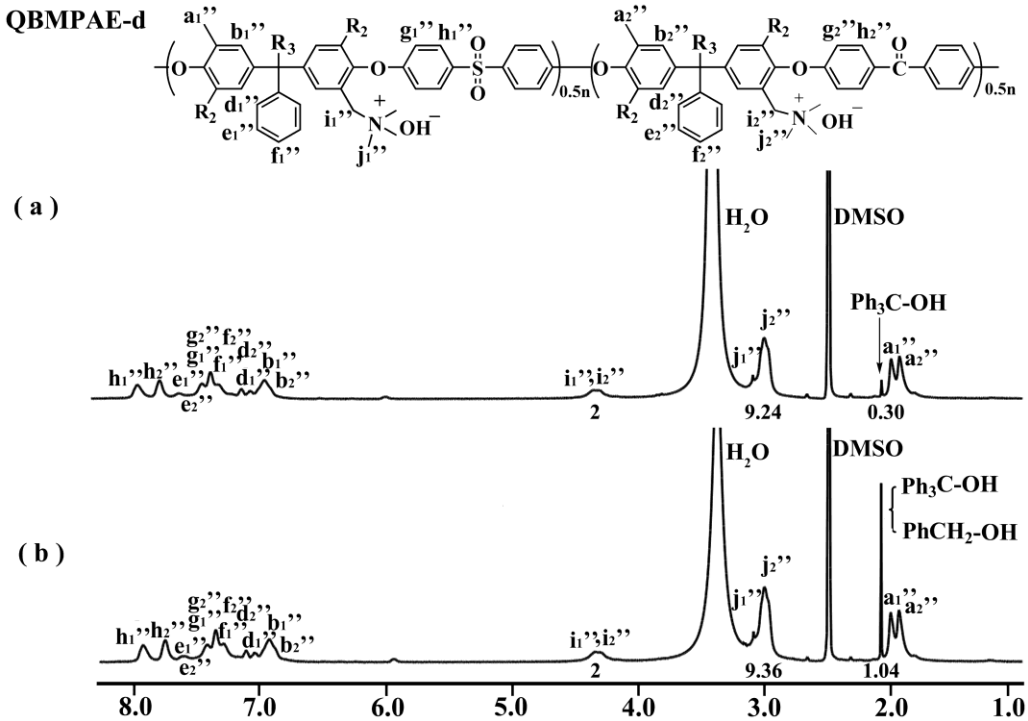

Fig. 5 The ^{1}H NMR spectra of the QBMPAE-**d** (IEC = 1.73 mmol g^{-1}) membrane (a) before and (b) after conditioning with 1 M NaOH at 60 ℃ for 168 h.

Table 7 Changes in the hydroxide conductivities of the QBMPAEs membranes after soaking in 1M NaOH at 60 °C for 168 h

Membrane	IEC[a] (mmol g^{-1})	Conductivity at 60 °C (mS cm^{-1})		
		Before stability test	After stability test	Decreasing amplitude (%)
QBMPAE-**a**	1.45±0.11	18.3±0.1	13.0±0.2	29.0
QBMPAE-**b**	1.71±0.15	27.2±0.3	16.2±0.1	40.4
QBMPAE-**c**	1.50±0.13	23.3±0.2	18.8±0.1	19.6
QBMPAE-**d**	1.73±0.15	32.0±0.2	26.5±0.2	17.3

[a]Experimental IEC for QBMPAEs membranes (OH^- from), determined using back titration.

Table 8 Changes in mechanical properties of the QBMPAEs membranes after soaking in 1 M NaOH at 60 °C for 168 h

Membrane	IEC[a] (mmol g^{-1})	Tensile strength (MPa)		
		Before stability test	After stability test	Decreasing amplitude (%)
QBMPAE-**a**	1.45±0.11	14.8±0.7	11.8±0.6	20.2
QBMPAE-**b**	1.71±0.15	9.2±0.5	6.9±0.2	25.0
QBMPAE-**c**	1.50±0.13	18.6±0.2	9.1±1.5	51.1
QBMPAE-**d**	1.73±0.15	10.9±0.1	6.5±0.1	40.4

[a]Experimental IEC for QBMPAEs membranes (OH^- from), determined using back titration.

51.1%. Arges has recently revealed the degradation mechanism in base for BPA-polysulfone-based anion exchange membranes using two-dimensional NMR spectroscopy, unequivocally demonstrating that cations trigger backbone degradation via quaternary carbon and ether hydrolysis.[41] Our QBMPAEs membranes had no quaternary backbone carbons. The loss of mechanical properties might have occurred because the quaternary benzyl ammonium groups initiated ether hydrolysis on the backbone. However, the QBMPAEs membranes show good mechanical properties after the alkaline stability test with tensile strengths over 6 Mpa.

When considering the IEC, water uptake, dimension stability, hydroxide conductivity, thermal stability and long term alkaline stability, the QBMPAE-**d** membrane is a potential AEM candidate. We investigated the alkaline stability of the QBMPAE-**d** under varying concentrations of NaOH at room temperature for 30 days. The conductivities of the QBMPAE-**d** (IEC = 1.73 mmol g^{-1}) at 60 ℃ after treatment were examined, as shown in Fig. 6. The hydroxide conductivity values of the treated QBMPAE-**d** membrane were higher than in the original membrane. The maximum hydroxide conductivity (53.9 mS cm^{-1}) was obtained at 6 M. The enhancement of hydroxide conductivities of the QBMPAEs membranes decreased after

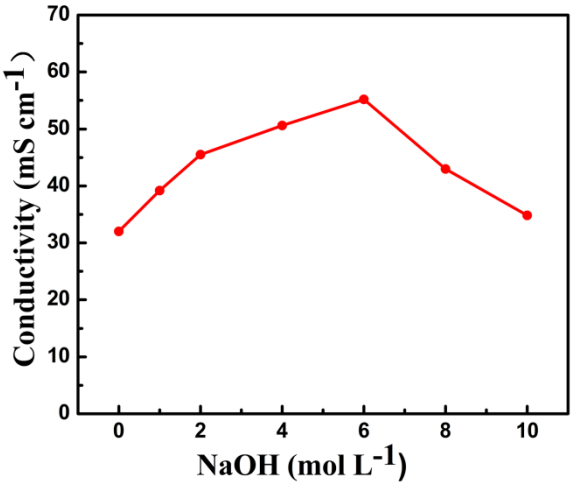

Fig. 6 Effect of the NaOH concentration on conductivity of QBMPAE-**d** (IEC = 1.73 mmol g^{-1}) after conditioning for 30 days.

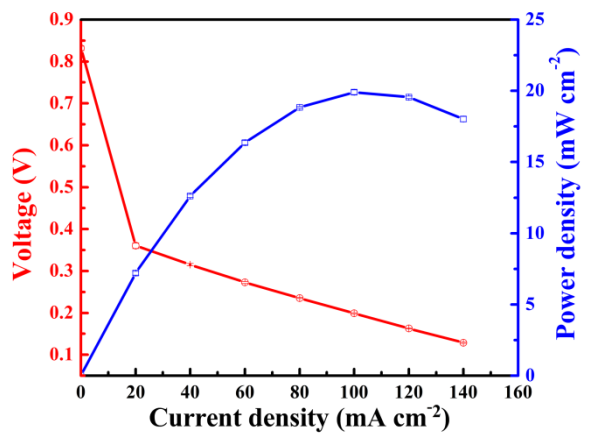

Fig. 7 Polarization and power density curves for the H_2/air single cell using QBMPAE-**d** as alkaline anion exchange membrane and catalyst ink glue at 70 ℃ under 30 psig; the Pt loading is 0.1 mg cm^{-2} for the anode and 0.2 mg cm^{-2} for the cathode.

further increases in NaOH concentration. This phenomenon contrasts with the reported data.[15, 42] Two types of opposing effects may explain this behavior: the positive enhancement and negative degradation of the functional groups for the OH^- ions transportation, where the positive enhancement of the hydroxide conductivities overwhelms the negative decrease of the hydroxide conductivities contributed by the degradation under basic conditions. The positive enhancement is mainly attributed to the enhanced functionalization of the membranes. Due to the higher NaOH concentrations during the alkaline stability tests, additional OH^- ions entered the ion transport channels of the membranes, rebuilding the equilibrium of the reversible ion exchange reaction and increasing the concentration of the OH^- counter anions. This effect enhanced the functionalization of the testing membranes. The hydrogen bond binding OH^- ions of aromatic alcohol hydroxyl groups may also contribute to this behavior. The lowest conductivity (33.8 mS cm^{-1}) was a little higher than the original value (32.0 mS cm^{-1}) and appeared after 10 M NaOH treatment for 30 days. The samples showed no visible changes after being shaken slightly and maintained their elasticity and toughness. The obtained QBMPAE-**d** membrane was very stable under various basic conditions at room temperature.

3.6 Single-cell performances

The MEA of the H_2/air single-cell was constructed with a 5wt% QBMPAE-**d** (IEC = 1.73 mmol g^{-1}) ethanolic solution as the catalyst ink glue and QBMPAE-**d** (thickness 80 μm, IEC = 1.73 mmol g^{-1}) as the OH^- exchanged electrolyte membrane. The inks were sprayed at defined 5 cm^2 areas on both sides of the QBMPAE-**d** membrane to form catalyst layers with Pt loadings of 0.1 mg cm^{-2} for the anode and 0.2 mg cm^{-2} for the cathode.The H_2/air single-cell performances of the MEA were investigated at 70 ℃ with fully humidified H_2 and air at the anode and cathode, respectively. The anode stream was hydrogen at 300 mL min^{-1}, and the cathode stream was air at 800 mL min^{-1}. The polarization and power density curves are shown in Fig. 7. The alkaline fuel cell exhibited an open circuit voltage (OCV) of 0.84 V, remaining similar to a fuel cell using a guanidinium functionalized GPPO-0.54 (thickness 80 μm, IEC = 2.69 mmol g^{-1}).[35] A peak power density of 20.1 mW cm^{-2} at 100 mA cm^{-2} was achieved. The cell performance of QBMPAE-**d** was similar to that of a QA PPO-based AEM at 70 ℃ (19.5 mW cm^{-2})[43] and much higher than that of a guanidinium functionalized GPPO-0.54 at 50 ℃ (16 mW cm^{-2}).[35] The performance was still low at the current stage due to the following two factors: (i) the very low Pt loading of the anode and cathode and (ii) the non-optimized MEA fabrication conditions. The results demonstrate that the prepared QBMPAE-**d** has potential AEMFC applications, although further improvements in power density are required.

4. Conclusions

A series of novel anion exchange membranes containing tetramethyl triphenyl methane moieties were synthesized via polycondensation, bromomethylation, quaternization, and alkalization. Under the optimized conditions, the obtained BMPAEs had DBM values up to 1.52 without visible side reactions. The conductivities of the QBMPAE membranes increased with water uptake and temperature. The hydroxide transport activation energy of the QBMPAEs membranes ranged from 8.01 to 10.24 kJ mol^{-1}. The highest hydroxide conductivities at 20 ℃ and 80 ℃ were 22.5 and 46.6 mS cm^{-1}, respectively; these values were demonstrated by the QBMPAE-**d** membrane with a IEC value of 1.73 mmol g^{-1}. The water uptake and swelling ratios of the obtained QBMPAEs membranes were moderate and can be adjusted by controlling their DBM values. Moreover, the QBMPAEs membranes exhibit good thermal stability and mechanical properties, as well as excellent hydroxide conductivity and alkaline stabilities. A power density of 20.1 mW cm^{-2} has been demonstrated by an alkaline membrane fuel cell operated at 70 ℃ using an entirely homemade MEA without any hot-pressing. These properties are promising for fuel cell applications.

Acknowledgements

This work was supported by the National Natural Science Foundation of China (NSFC) (Grant 51173045), the Research

Fund of the Key Laboratory of Fuel Cell Technology of Guangdong Province (Grant 201104), the Funds of the National College Students' Innovative Entrepreneurial Training Plan (Grant 201210561055-2601) and the Guangdong Province College Students' Innovative Entrepreneurial Training Plan (Grant 1056112040-405).

References

1. B. C. H. Steele and A. Heinzel, *Nature*, 2001, 414, 345-352.
2. G. Couture, A. Alaaeddine, F. Boschet and B. Ameduri, *Prog. Polym. Sci.*, 2011, 36, 1521-1557.
3. H. Sun, G. Zhang, Z. Liu, N. Zhang, L. Zhang, W. Ma, C. Zhao, D. Qi, G. Li and H. Na, *Int. J. Hydrogen Energy*, 2012, 37, 9873-9881.
4. F. Bidault, D. J. L. Brett, P. H. Middleton, N. Abson and N. P. Brandon, *Int. J. Hydrogen Energy*, 2009, 34, 6799-6808.
5. R. K. Nagarale, V. K. Shahi and R. Rangarajan, *J. Membr. Sci.*, 2005, 248, 37-44.
6. Y. Wu, C. Wu, Y. Li, T. Xu and Y. Fu, *J. Membr. Sci.*, 2010, 350, 322-332.
7. Y. Wu, C. Wu, F. Yu, T. Xu and Y. Fu, *J. Membr. Sci.*, 2008, 307, 28-36.
8. R. Vinodh, M. Purushothaman and D. Sangeetha, *Int. J. Hydrogen Energy*, 2011, 36, 7291-7302.
9. X. Li, Y. Yu and Y. Meng, *ACS Appl Mater Interfaces*, 2013, 5, 1414-1422.
10. T. Zhou, J. Zhang, J. Qiao, L. Liu, G. Jiang, J. Zhang and Y. Liu, *J. Power Sources*, 2013, 227, 291-299.
11. J. Zhang, J. Qiao, G. Jiang, L. Liu and Y. Liu, *J. Power Sources*, 2013, 240, 359-367.
12. T. Zhou, J. Zhang, J. Jingfu, G. Jiang, J. Zhang and J. Qiao, *Synth. Met.*, 2013, 167, 43-50.
13. D. W. Seo, M. A. Hossain, D. H. Lee, Y. D. Lim, S. H. Lee, H. C. Lee, T. W. Hong and W. G. Kim, *Electrochim. Acta*, 2012, 86, 360-365.
14. X. Li, Y. Yu, Q. Liu and Y. Meng, *Int. J. Hydrogen Energy*, 2013, 38, 11067-11073.
15. X. Li, Y. Yu, Q. Liu and Y. Meng, *ACS Appl Mater Interfaces*, 2012, 4, 3627-3635.
16. M. R. Hibbs, M. A. Hickner, T. M. Alam, S. K. McIntyre, C. H. Fujimoto and C. J. Cornelius, *Chem. Mat.*, 2008, 20, 2566-2573.
17. L. Li and Y. Wang, *J. Membr. Sci.*, 2005, 262, 1-4.
18. G. Wang, Y. Weng, D. Chu, D. Xie and R. Chen, *J. Membr. Sci.*, 2009, 326, 4-8.
19. H. Zhang and Z. Zhou, *J. Appl. Polym. Sci.*, 2008, 110, 1756-1762.
20. H. Zarrin, J. Wu, M. Fowler and Z. Chen, *J. Membr. Sci.*, 2012, 394-395, 193-201.
21. W. Ma, C. Zhao, H. Lin, G. Zhang and H. Na, *J. Appl. Polym. Sci.*, 2011, 120, 3477-3483.
22. Z. Liu, X. Li, K. Shen, P. Feng, X. Xu, W. Hu, Z. Jiang, B. Liu and M. Guiver, *J. Mater. Chem. A*, 2013, 1, 6481-6488.
23. K. Shen, J. Pang, S. Feng, Y. Wang and Z. Jiang, *J. Membr. Sci.*, 2013, 440, 20-28.
24. M. R. Hibbs, C. H. Fujimoto and C. J. Cornelius, *Macromolecules*, 2009, 42, 8316-8321.
25. G. Liu, Y. Shang, X. Xie, S. Wang, J. Wang, Y. Wang and Z. Mao, *Int. J. Hydrogen Energy*, 2012, 37, 848-853.
26. R. Vinodh, A. Ilakkiya, S. Elamathi and D. Sangeetha, *Mater Sci Eng B-Adv*, 2010, 167, 43-50.
27. X. Lin, X. Liang, S. D. Poynton, J. R. Varcoe, A. L. Ong, J. Ran, Y. Li, Q. Li and T. Xu, *J. Membr. Sci.*, 2013, 443, 193-200.
28. X. Lin, L. Wu, Y. Liu, A. L. Ong, S. D. Poynton, J. R. Varcoe and T. Xu, *J. Power Sources*, 2012, 217, 373-380.
29. J. R. Varcoe, R. C. T. Slade, E. L. H. Yee, S. D. Poynton, D. J. Driscoll and D. C. Apperley, *Chem. Mater.*, 2007, 19, 2686-2693.
30. D. Chen and M. A. Hickner, *ACS Appl. Mater. Interfaces*, 2012, 4, 5775-5781.
31. T. Xu and W. Yang, *J. Membr. Sci.*, 2001, 190, 159-166.
32. J. Yan and M. A. Hickner, *Macromolecules*, 2010, 43, 2349-2356.
33. X. Li, Q. Liu, Y. Yu and Y. Meng, *J. Mater. Chem. A*, 2013, 1, 4324-4335.
34. L. Wang, Y. Z. Meng, S. J. Wang, X. Y. Shang, L. Li and A. S. Hay., *Macromolecules*, 2004, 37, 3151-3158.
35. X. Lin, L. Wu, Y. Liu, A. L. Ong, S. D. Poynton, J. R. Varcoe and T. Xu, *J. Power Sources*, 2012, 217, 373-380.
36. J. G. Speight, *Lange's Handbook of Chemistry*, McGraw-Hill, New York, sixteenth edn., 2005.
37. G. Merle, M. Wessling and K. Nijmeijer, *J. Membr. Sci.*, 2011, 377, 1-35.
38. B. Lin, L. Qiu, J. Lu and F. Yan, *Chem. Mater.*, 2010, 22, 6718-6725.
39. M. Tanaka, M. Koike, K. Miyatake and M. Watanabe, *Polym. Chem.*, 2011, 2, 99-106.
40. B. C. Lin, L. H. Qiu, B. Qiu, Y. Peng and F. Yan, *Macromolecules*, 2011, 44, 9642-9649.
41. C. G. Arges and V. Ramani, *P.N.A.S*, 2013, 110, 2490-2495.
42. G. Wang, Y. Weng, D. Chu, R. Chen and D. Xie, *J. Membr. Sci.*, 2009, 332, 63-68.
43. A. L. Ong, S. Saad, R. Lan, R. J. Goodfellow and S. W. Tao, *J. Power Sources*, 2011, 196, 8272-8279.

